Fractional Distillation of Bio Medical Waste Plastic Pyrolysis Oil Blend N-Butanol With Nano Graphene Oxide Additive Emulsion On CRDI Diesel Engine Performance

Rajkumar. P[1] B. Prem Anand[2],

Engine Research Laboratory
[1,2,3,4] FEAT, Department of Mechanical Engineering, Annamalai University
Annamalai Nagar – 608 002, Tamilnadu
rajkumarme2014@gmail.com, prem.au2005@gmail.com, rsdk66@yahoo.com

Abstract

This study aims to develop a enhance thermal cracking with catalyst activate technique under oxidizing circumstances to convert plastic-based medical wastes into liquid fuel oil.. High-density polyethylene medical waste with Neyvely Lignite Flay Ash catalyst produced bio medical plastic pyrolysis oil and fractional distillation column process. A customised common rail direct injection (CRDI) diesel engine uses PPO, diesel, n-butanol, and GO nanoparticles to improve performance, combustion, symmetric characteristics, and emissions. Probe sonication was used to dissolve different amounts of GO nano-additive, which contains asymmetric graphene oxide and sodium dodecyl benzene sulphonate (SDBS) emulsifier, in 10% n-butanol. Four stable and symmetric nanofuel mixes were created from graphene oxide at 30, 60, 90, and 120 ppm. This experiment used nanofluid, plastic pyrolysis oil, and n-butanol. Thermogravimetric and Fourier transform infrared spectroscopy examined plastic pyrolysis oil nanofuel combinations. PPO20B10GO90 nanofuel. Increasing fuel injection pressure from 300, 600, and 900 bar with pilot injections improved. NOx emissions fall and CO emissions rise with engine load. Engine load decreases unburned hydrocarbon emissions, but waste plastic oil mixtures increase them. For most full loads and mixtures, PPO20B10GO90 produces less CO2 than diesel.

Keywords: *Bio Medical Waste Plastic pyrolysis oil, Graphene oxide Nanoparticles, CRDI Engine, n-butanol*

1. Introduction

Heat waste plastics at 300–400°C for 3–4 hours with 1 wt.% catalyst and 10 wt.% coal under air pressure to fuel. Tests showed that the liquid in the engine could produce 75%. A single-cylinder, four-stroke, air-cooled diesel engine was employed for the experiments, which ran at 1500 rpm with 4.4 kW load. Physical and chemical properties of test fuels: dense, consistent, high-temperature-value[1] Since HDPE has a limited lifespan, more of it has been discarded as its use and production have increased. Already recycling plastics.massively occurring. Pyrolysis is the best chemical feedstock recovery method [2]. Heat without oxygen degrades polymers in thermal cracking or thermal pyrolysis. Scholars [3-5] have examined how reactor design and temperature affect HDPE pyrolysis. Optimised HDPE thermal breakdown catalysts can boost byproduct yield. For this process, zeolite, alumina, silica-alumina, FCC catalyst, and reforming catalyst are popular [6-12]. An inert atmosphere can pyrolyze waste plastics into wax, liquid, and gas. Liquids with chemical feedstock or fuel properties are more appealing. Numerous studies have examined the production of oil from waste plastic [13,14]. In compression ignition engines, waste plastic oil competed with petroleum [15]. Diesel and other compression ignition engines are the most used power plants due to their manoeuvrability and thermal efficiency.

Their health risks from high NOx and smoke levels outweigh their benefits. Thus, diesel engine fuel alternatives are needed due to strict emission requirements and petroleum fuel depletion [16-21]. Oil demand is rising due to the growing number of cars.

Oil demand is rising due to the growing number of cars. Pilot and high-pressure injection reduce NOx emissions by 35% and smoke emissions by 60-80% without affecting fuel efficiency [17]. Since shorter combustion periods near TDC improve efficiency, studies with 3 CA degree injection spacing showed lower BSFC than those with 8 CA degree spacing. Split injection lowers NOx and increases particle emissions, according to studies. By continuing combustion into the expansion stroke and decreasing soot, split-injection reduces emissions. Optimisation of injection features to encourage mixing may lower particle emissions compared to single-injection [18]. Pilot/main diesel fuel injection, Erhard Sitter et al. Pilot injection is positively displaced by a hydraulic pilot injection auxiliary pump piston driven by a high-pressure injection pump. The high-pressure injection pump first targets a storage piston in the main injection zone. Fuel storage piston line only on pilot injection piston stroke [19]. Cheap fuel additives can lower diesel pollution emissions. Nanomaterials may be eco-friendly diesel fuel additives, say researchers. Nanoparticles distribute liquid fuel uniformly. Higher surface-to-volume ratio[20,21].Recent investigations of diesel fuel additives suggest that active metal nanoparticles may enhance fuel economy and pollutants. Diesel and biodiesel with Al2O3 and CeO2 nanoparticles reduce pollutants and increase engine efficiency. Nanoparticles of Al2O3 in diesel fuel accelerate combustion[22]. Bio diesel with 20–80 ppm CeO2 reduced PM, CO, and NOx emissions and enhanced brake thermal efficiency. Nanoparticles of cerium oxide minimise hydrocarbon and NOx emissions[23]. Airborne metal oxide combustion byproducts may irritate the lungs and skin [24,25]. The chemical, physical, and combustion properties of graphite oxide make it a diesel-fuel additive. Carbon-oxygen-hydrogen (GO). GO nanostructures are oxygen-modified

2-D graphene sheets.[26,27]. Graphite oxidises three ways. Brodie and Staudenmaier oxidised graphite with KClO3 and HNO3, while Hummers used KMnO4 and H2 SO4. Intercalating graphite with strong acids like H2 SO4, HNO3, or HClO4 produces GO[28] precursor molecules. [28]. The engine performance rose by 6%, bsfc by 20%, NOx by 40%, CO by 60%, and UHC by 50% at 50 mg/L GNP. [29]. GO at 50 mg/L increases engine performance most (pmax. up 5%, bsfc down 17%, NOx down 15%, CO down 60%, etc.). [30].,Exothermic heat release from SWCNTs and GO in SDD and GDD fuels raised in-cylinder temperatures and heat release rates, increasing NOx levels compared to diesel. GDD and SDD emit 9.2% more NOx than diesel. Selective catalytic reduction or lean NOx traps lower NOx.SFC B20G90 decreases 14.48% with GO [31]. Ailanthus altissima biodiesels with nanoparticles lower CO emissions by 18% for B10G90 and UHCs by 27.47% for B20G90. Adding graphene oxide (GO) to biodiesel increases CO2 emissions by 12.54 percent and NOx emissions by 7.93 percent [32]. In another study, 50 mg/l MWCNTs added to 40% n-butanol (JME40B) fuel reduced CO, NOx, and UHC emissions by 65%, 70%, and 50% compared to pure D100 fuel [33]. Even at a 10% mix and lower speeds, n-butanol increases NOx emissions. The second WHSC mode (100% load and 55% speed) had the highest NOX emissions due to the SCR's lower operating temperatures at full load, with n-butanol mix emitting the most [34].

However, butanol reduced exhaust gas temperature and nitrogen oxide emissions. At full load, Bu10, Bu20, Bu30, Bu40, and Bu50 blends had 3.1%, 4.3%, 7.3%, 10.6%, and 13.5% lower NOx emissions than diesel [35]. The DI-CI engine performed better with a 20% butanol blend than diesel fuel, resulting in reduced emissions. In particular, a compression ratio of 19.5, fuel injection pressure of 210 bar, and fuel injection time of 230 CA bTDC decreased emissions and enhanced performance over diesel fuel operation [36]. Biodiesel-butanol blends of 5%, 10%, and 20% increased brake specific fuel consumption (BSFC), CO, and HC emissions while decreasing NOx and exhaust gas temperature in a small diesel engine. Butanol boosted biodiesel CO emissions [37].

Biodiesel-diesel mixes with n-butanol and diethyl ether have different engine performance and emissions. In biodiesel-diesel blends with 10% n-butanol, smoke emissions dropped 27%, NOx emissions 8.8%, and CO emissions 30.7%. A 10% n-butanol-biodiesel-diesel ternary had a 3.9% lower BSFC than a 20% biodiesel blend [38]. Diethyl ether decreased combustion temperatures and increased expansion stroke temperatures more than ethanol and n-butanol diesel fuel blends, while biodiesel or vegetable oil diesel fuel had little effect. Renew reaction NOx emissions are reduced by biofuel in diesel fuel. Mixing diesel and diethyl ether reduces pollutants. CO comes from biodiesel. Alcohol and diethyl ether mixtures increase unburned HC emissions, although vegetable oil or bio-diesel diesel fuel can lower them [39]. Butanol enhanced BSFC, NOx, and CO in vegetable oil-diesel (20:70) and decreased CO2 and HC. Ternary pairings can affect engine performance [40,41,42]. Graphene oxide nanoparticles in dairy scum oil biodiesel boosted brake thermal efficiency (11.56% for DSOME2040) and fuel consumption (8.34%). NOx emissions from nano fuel blends rose with viscosity, oxygen, flame temperature, and cetane. NOX fell 5.62% Best was B20 DSOME. Biodiesel any source increased NOx [43]. Graphene oxide (GO) nanoparticles in diesel/biodiesel blends reduced VOC, CO, and BSFC but increased NOx. Biodiesel from

camelina boosts power. [44]. found that biodiesel containing GO nano-particles reduced CO and UHC emissions but increased CO2 and NOx emissions. The lowest CO output is B20GO90 at full load. Biodiesel with GO nanoparticles may improve engine performance and reduce pollutants. Reduced emissions with GO nanoparticles. [45] High surface-to-volume ratios and oxygen-reactive regions characterise GO. The linear burn-rate and ignition temperature of liquid monopropellant nitromethane increased with decreasing graphene sheets. 29 Based on these findings, we conduct a single droplet experiment to evaluate GO-dosed diesel fuel's combustion characteristics and environmental impact. [46].

Diesel blends with 75% transesterified mahua oil were most efficient. Transesterified mahua oil improves 25% diesel thermal efficiency. [47] .All 10%–30% blends release less NOx than diesel. Sulphur-free alcohols burn without soot. Diesel engines powered by alcohol should not emit particulates. Diesel emits more particles than methyl esters. Diesel PM exceeded 10%, 20%, and 30% mixtures. Diesel engines can use 30% MOME and 70% conventional diesel. [48] Triglyceride and alcohol become glycerol and ester with a catalyst. Low-viscous ester molecules are one-third the size of oil molecules. A 3:1 alcohol-to-triglyceride ratio is needed for transesterification. High-conversion, low-viscosity biodiesel has a higher alcohol-to-oil ratio. [49,50]

Vegetable oil-based compression ignition engine fuels increased production and consumption. History, current and projected crop yields, vegetable oil conversion to diesel fuel technology and economics, oil performance, diesel fuel coproduction, environmental factors, and future research will be covered. We won't replace diesel with vegetable oils. At 0.1% and 0.01% dosing levels, graphite oxide (GO) nanoparticles with Al2O3 and CeO2 nanoparticles improved diesel fuel combustion and reduced diesel engine pollution emissions. As a diesel fuel additive, GO may reduce pollution and fossil fuel depletion. [52]. CO2, HC, smoke, and CO emissions from Nigella sativa lowered by GO NPs. The maximum load smoke, HC, and CO emissions of NSME25B10GO90 were 31.68%, 48.571%, and 50.15% lower than NSME25. [53].

Aqueous sodium dodecylbenzene sulfonate solution contains 28-65%, 6-8% alkali, 0-8% cosolvent, 0-1% additive, and water. Invention produces aqueous sodium dodecyl benzene sulfonate. [54]. We compared SME20 graphene dispersions to two standard surfactants at optimal concentration by absorbance. Nanofluid UV–Vis detection of graphene. Any surfactant concentration decreased nanofluid absorbance with static time using UV–Vis spectral method. Simarouba biodiesel-diesel mixtures are 1:4.

Dispersion is maintained by graphene-surfactant ratio. SDBS dissolves graphene better than SDS in Simarouba diesel biodiesel blends[55]. Small amounts of colloids in liquid hydrocarbon fuels have been employed to improve ignition and performance[56,57].

Biomedical waste is solid and liquid. Plastic-based medical wastes often consist of solid items such as vials, syringes, infusion sets, pipes, covers, pharmaceutical containers, and packs. Medical waste is harmful and infectious, posing a significant environmental danger. Proper treatment and management are necessary before disposal. Medical waste can cause diseases and ailments on people by direct contact or environmental contamination of air,

water, and soil. Consequently, improper medical waste management puts society and the environment at risk[62].

Medical wastes are managed by segregation, disinfection, storage, transportation, collection, disposal in landfills or recycling. In medical waste management, various recycling methods are used, various recycling methods are used, including biological, mechanical, and thermo-chemical recycling [62].

2. Motivation and research goals

Bio medical waste plastic pyrolysis distillation oil with catalyst as a Neyvely Lignite Flay Ash was modified by being re-fuxed with a 3 N NaOH or 3 N H_2SO_4 solution enhance to pyrolysis of process to waste plastic fuel blend with GNP and n-butanol diesel additives improved CO, HC, and NOx combustion and emissions in earlier study. Previous research ignored fuel-additive blend smoke fluctuations because compression ignition engines have a NOx-to-smoke ratio concern. GO and GNP are compared to diesel, PPO mixes, and fuels for combustion, smoke emissions, friction, and filtering. Different fuel injection pressures and GNP additives for diesel and PPO combustion and emissions.

3. Pyrolysis of Bio medical Waste Plastic

3.1 Description of Pyrolysis of Bio medical Waste Plastic to fuel Plant

Schematic of waste plastic withe catalyst conversion plant in Fig.4.3. The reactor has a 1300 mm stainless steel cylindrical vessel. The reactor has three electrical coils. Coils are 1.5 kW. These coils heat the reactor. Small cylindrical sheet surrounds reactor. Between the reactor vessel and thin sheet is glass wool. Glass wool makes insulation. Top of reactor has stirrer, safety valve, pressure gauge, inlet with air-tight stop cock for waste plastic, and output to water-cooled condenser. Safety valves tolerate 500 kg/m^2 pressure. Electricity slows the stirrer. The stirrer helped mix the catalyst and waste plastic and maintain temperature. On the reactor bottom is a hand hole with an airtight stop cock to remove cracked materials. To measure reactor temperature, a thermocouple is put at the bottom. Temperature indicator and controller with switches are on the control panel. A reactor temperature indicator reveals its temperature. Controllers regulate reactor temperatures.

Condensers have cooling coils and water jackets. Stainless steel coils of 1800 mm length and 20 mm diameter make up the condenser. The water jacket holds this 300-mm-diameter, 500-mm-tall coil. Bottom and top inlets and outlets are on the water jacket. Inlet and outflow circulate water in the jacket. Stainless steel tanks collect condensed oil. Uncondensed gas is routed through an AVL di-gas analyzer to the flame arrester to prevent backfire. Gas analysers measure uncondensed hydrocarbon evaluation rates. A glass water vessel is the flame arrester. Burner-connected flame arresters release gasses into water.

3.2 Activation of fy ash by alkalis and acids

Neyvely Lignite Flay Ash was modified by being re-fuxed with a 3 N NaOH or 3 N H_2SO_4 solution [61]. The mufe furnace was used to dry the treated solids at 120 degrees Celsius and

calcine them for four hours at 550 degrees Celsius. BFA and AFA are the abbreviations for these two types of samples.

In pyrolysis, the feedstock is bio medical waste plastic with Neyvely Lignite Flay Ash was modified by being re-fuxed with a 3 N NaOH or 3 N H_2SO_4 solution cat/pol = 0.20 (A and B) as a catalyst heated to a temperature at 350 ℃ a specific heating rate and then kept there for an established amount of time without the presence of oxygen. Reactions include depolymerization, dehydration, decarbonylation, decarboxylation, deoxygenation, oligomerization, and aromatization occur during pyrolysis to break down big hydrocarbon molecules into relatively smaller ones. Many parameters, including, pyrolysis temperature, heating rate, and the catalyst effect, affect the total and relative amounts of pyrolysis products. The output of pyrolysis oil increases when a biomass feedstock is heated rapidly, and the resulting vapors condense quickly, according to research conducted.

4. Fractional Distillation of Plastic Oil

The plastic oil was poured through the inlet of the distillation unit. After pouring the oil, the valve was closed tightly. In the control panel the temperature was set for collecting first fraction boiling within 100 ℃. After checking the silicone oil level and the flow of water in the condenser the electrical heater was switched ON. As the coil gets heated the heat was transferred to the silicone oil that leads to a rise in temperature of the silicone oil. Increase in the temperature of the silicone oil also increased the temperature of the plastic oil.

As the temperature rose the plastic oil vaporized and the vapour was passed into water cooled condenser. In the condenser the vapour was converted into liquid. This oil was collected in a jar. This oil was collected in the same jar till the catalytic oil reaches the fractionated set temperature. The electrical coil switched OFF automatically when the plastic oil reached the set temperature.

After this the set temperature in the control panel was increased to 150℃ for collecting the second fraction. As the set temperature increased the electrical heating coil switched ON automatically which leads to a rise in temperature of the catalytic oil. The vapour formed was passed to the condenser. The condensed fractionate oil was collected in a different jar. The same procedure was adapted to obtain the third and fourth fractions of oil boiling in the range 150 – 200 ℃ and above 200℃.

5. Experimental setup

Kirloskar AV1, a single-cylinder diesel engine having Common Rail Direct Injection, water cooling, and four valves per revolution. The engine had 3.7 hp. While injector pressures ranged from 300 to 900 bar, the engine ran at 1500 rpm. A stable engine speed for pressure required 650-1200 microseconds of fuel injection. Engine specs are in Table 2 and fuel injector specs are in Table 3. The experimental setup schematic is in Figure 2, and the common-rail schematic is in Figure 3.

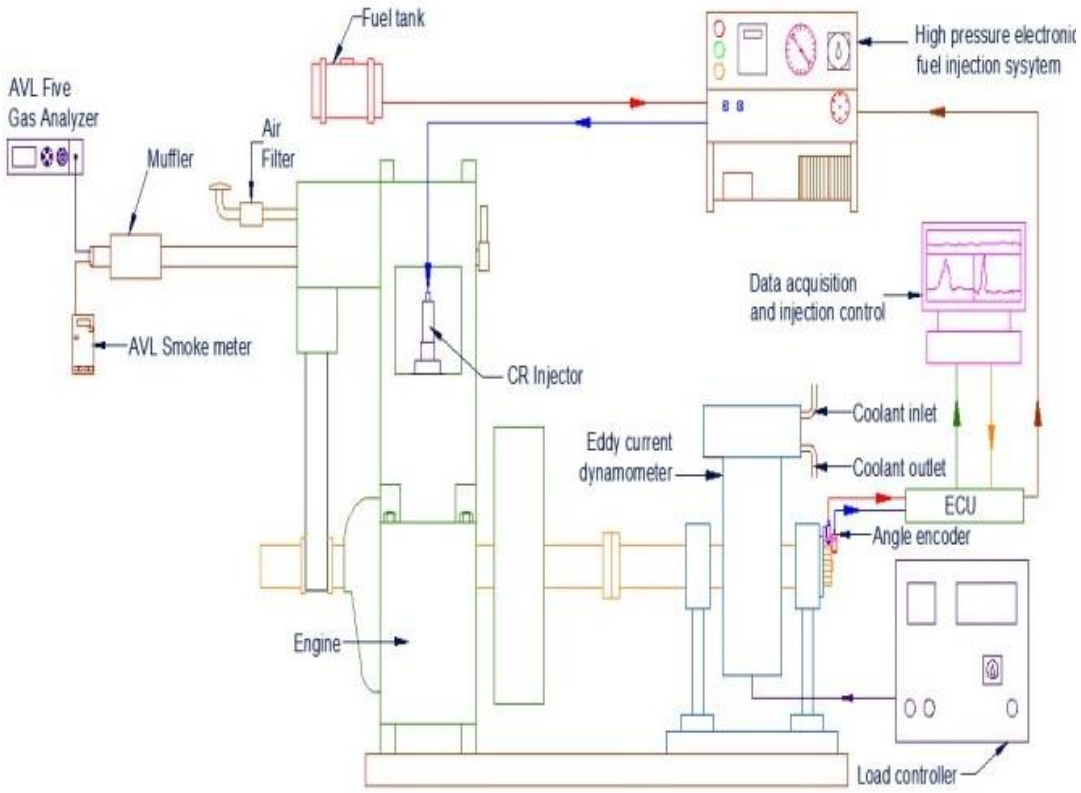

Fig. 2. CRDI Experimental setup

Type	CRDI engine with a single cylinder, vertical orientation, water cooling, and four strokes.
Brand	Kirloskar Engine
Power	3.7 kW
Stroke	110 mm
Bore	80 mm
Speed	1500 rpm
Compression ratio	17.5:1
Injection pressure	Variable from 300 bar, 600bar, 900bar
Mode of starting	Manually cranking
Orifice diameter (Air mass flow measurement)	20 mm

Table 2 Engine specifications

The high-pressure side was prototyped with one injector and a mass-produced Kirloskar pump.A 1500-rpm engine. The high-pressure zones fuel pump was run independently of the engine's highest level to maximise injection-pressure range.

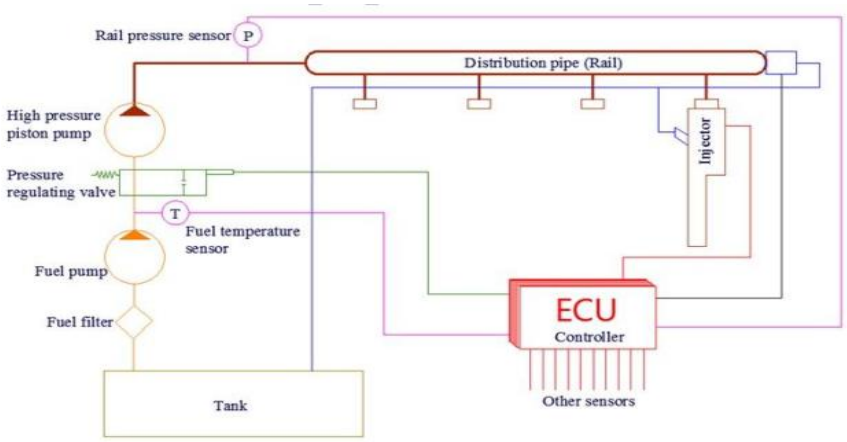

Figure 3 depicts a common-rail schematic design.

Fuel fed	Units	Common rail
Injection pressure	MPa	20-100
The total number of holes in the nozzle	-	3
Diameter of the nozzle hole	Mm	0.518
Initial Injection Start	-	23º Before top dead centre (BTDC)
Amount of time needed for an injection	µsec	650-3000

Table 3 Fuel injector system specification

A production input metering valve is used to pressurise only the necessary amount of petrol for injection. Pressure is regulated by high-frequency signals on injector spill valves. Since no 16-bit controller or spill flow was available, a rail-mounted high-pressure valve handled fuel pressure. Its usefulness relies on filtering. Using filter paper darkness, reflecting photometers calculate HSUs. Researchers used AVL Digas gas analyzer. System accuracy was 2% and linearity +/-1% over 8 hours.

6. Graphene oxide (GO)

Graphene is hexagonal carbon. Two-dimensional graphene. Heat and electricity flow best through graphene. Electronics, medications, PPO fuel additives, aeroplanes, and more use graphene.

Due of graphene's high cost and intricate manufacture, researchers are seeking cheaper alternatives with equivalent benefits. Graphite, a cheap and abundant material, is oxidised into GO, a 1-atomic-layer molecule. Graphene oxide contains oxygen. Graphene is easy to manipulate when distributed in water or other solvents. Conductivity can be increased in graphene oxide. Powder, liquid, PPO fuel additive of varying parts per million, and coating are common types.

7. Stability of Nanoparticles

Particle aggregation threatens dispersed nanofluid sustainability. Due to Van der Waals forces, nanoparticles will recombine without ultrasonic energy. Repulsion (steric, electrostatic, or electrosteric) or a comparable refractive index can prevent recombination. Particles agglomerate when attraction exceeds repulsion. Repulsion over attraction prevents particle aggregation and maintains stability. This study used ultrasonication and magnetic stirrer high-shear mixing. Physical dispersion and chemical surface functionalization with surfactants prevent continuous phase solvent agglomeration [58]. Electrostatic and steric interactions stabilise surfactants. Repulsion keeps surfactant-coated nanoparticles apart [59].

SDBS is a high-anionic surfactant that deters, moistens, foams, emulsifies, and disperses. SDS/SDBS surfactant adjustments for graphene oxide dispersion. A specific surfactant-graphene oxide ratio optimises dispersion.

8. Combination of Fuel Components

In this study, graphene oxide nanoparticles are dispersed in a solution of SDBS surfactant and distilled water using a probe sonicator. Ultrasonicating and NPs with 10% n-butanol may improve the oxygen concentration of biodiesel. At 30, 60, 90, and 120 mg/L, graphene oxide nanoparticles are added to fuel mixtures using a magnetic stirring device, ultrasonicator bath, and probe sonicator. Graphene oxide NPs (30 ppm) and SDBS surfactant (15 ppm) are both found in the PPO20B10GO30 fuel blend. Combination of PPO20B10GO60 and 60 ppm GO NPs in an SDBS surfactant at 25 ppm. To create PPO20B10GO90 and PPO20B10GO120, PPO20 biodiesel is mixed with either 90 or 120 ppm graphene oxide nanoparticles and either 35 or 45 ppm SDBS surfactant, respectively. The components of nanofluids are SDBS surfactant, graphene nanoparticles, and 5 ml of distilled water. Then, for the next twenty to thirty minutes, these parts will be exposed to ultrasonic waves at a frequency of twenty kilohertz.

By disturbing the symmetry of particles and dissolving intermolecular interactions, sonication hinders the formation of aggregates. After adding the nanofluids to the PPO20 biodiesel, the mixture is heated to 60 degrees Celsius, stirred with a magnetic agitator for 15 minutes to remove moisture and water, blended in a bath-type sonicator for an hour, and then sonicated in a probe sonicator to improve nanoparticle stability. These techniques could be used to produce stable nanofuel mixtures. Physiochemical features of fuel blends.

Properties	Unit	ASTM Standard (D6751-15C)	Diesel	PPO20	PPO20B10GO90
Kinematic Viscosity	cSt @ 40 ℃	ASTMD445	2.35	3.789	2.912
Calorific Value	MJ/kg	ASTM D5865	45.458	41.98	43.89
Density	Kg/m^3 @	ASTM D4052	822.89	844.89	844.95

	15 ℃				
Specific Gravity	gm/cc	ASTM D891	0.8	0.838	0.832
Flash point	℃	ASTMD93	78	112.59	98.54
Four Point	℃	ASTM D97-12	-4	3.1	2.01
Cloud Point	℃	ASTM D2500-11	-1	5	5.41
Cetane Number	-	ASTMD 613	49.52	45.56	52.12

Table 4 Physiochemical traits associated with diesel, Pyrolysis fuel oil and nanofuel blends

9. Evidence for the involvement of fly ash as catalyst

The observations made on the degradation of HDPE definitely show that fly ash functions as a catalyst in the degradation of HDPE. A catalyst may undergo a physical change during the reaction in which it acts as a catalyst. However, it does not undergo any permanent chemical change. Its chemical nature is not altered after the reaction. The change in the physical nature can be detected by using SEM images. The 40 μm, SEM images of the raw fly ash remaining after the reaction for cat/pol = 0.20 are shown in Fig 4. The 40μm SEM images for other cat/pol ratios and SEM images corresponding to 20 μm, 5 μm, 4 μm and 2 μm.

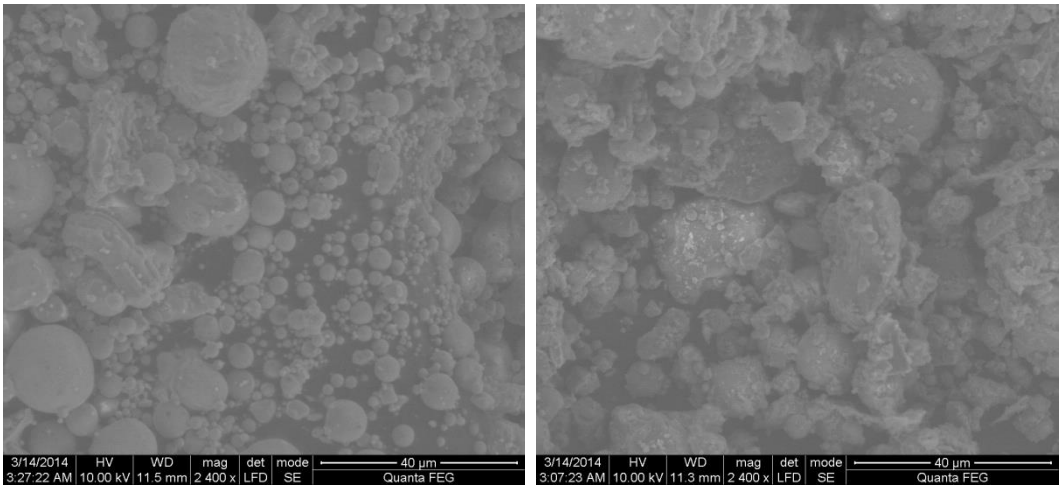

Fly Ash (A) HDPE (B)

Figure 4. 40 μm SEM images of raw fly ash (A), materials reaming after degradation of HDPE and cat/pol = 0.20 (A and B)

From the images shown in Fig it is clear that physical nature of fly ash is changed during the degradation.

The EDX spectrum of raw fly ash is compared with those for fly ash obtained after degradation of HDPE and for cat/pol = 0.20 in Plates 1, 2 and 3. The EDX

spectra of the fly ash obtained for the other cat/pol ratios. Examination of EDX spectra in Plates 1, 2 and 3 and those in the Appendix 5 clearly shows that the peaks for Si, Al and O are not affected by the degradation. This shows that fly ash does not undergo a permanent chemical change during the degradation of HDPE.

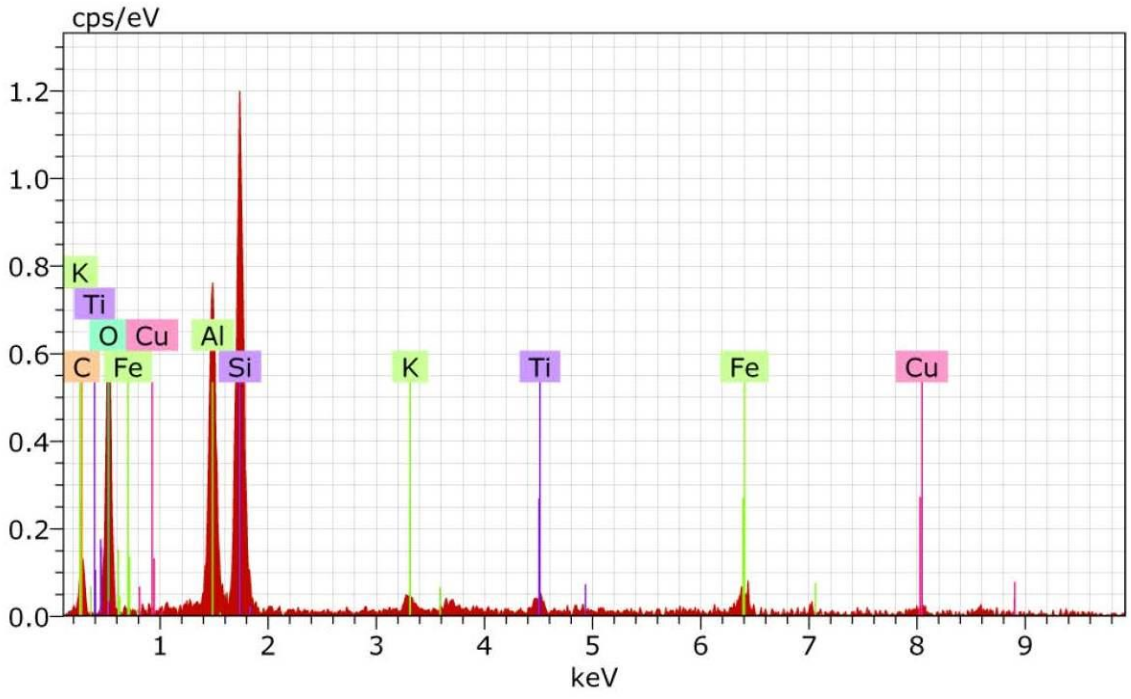

Plate 1 EDX Spectrum of Fly ash

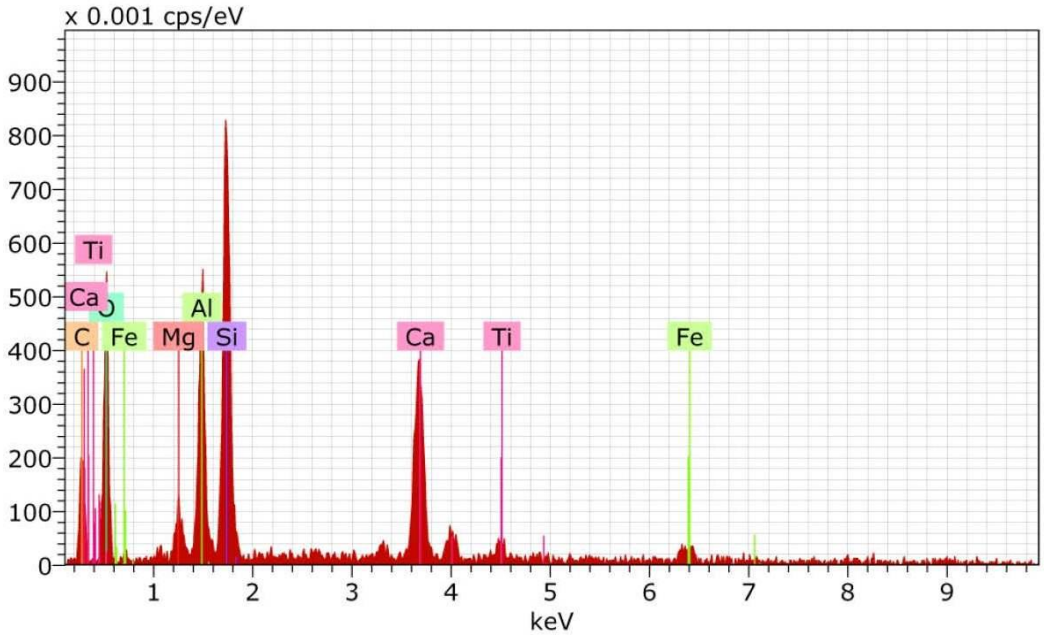

Plate 2 EDX spectrum of fly ash remaining after degradation of HDPE using cat/pol = 0.20

10. Fourier transforms infrared analysis

The FT-IR spectrum model. Figures 5 and 6 show diesel and PPO20B10GO90 Nanofuel FTIR spectra. Alcohol is detected in the electromagnetic spectrum of PPO20B10GO90 Nanofuel mixed fuel by strong O-H band stretching vibrations between 3700 and 3550 cm-1. Band between 3700 and cm-1. Both test fuels have a dominant peak between 3000 and 2800 cm-1. This peak represents alkane C-H stretching vibrations.

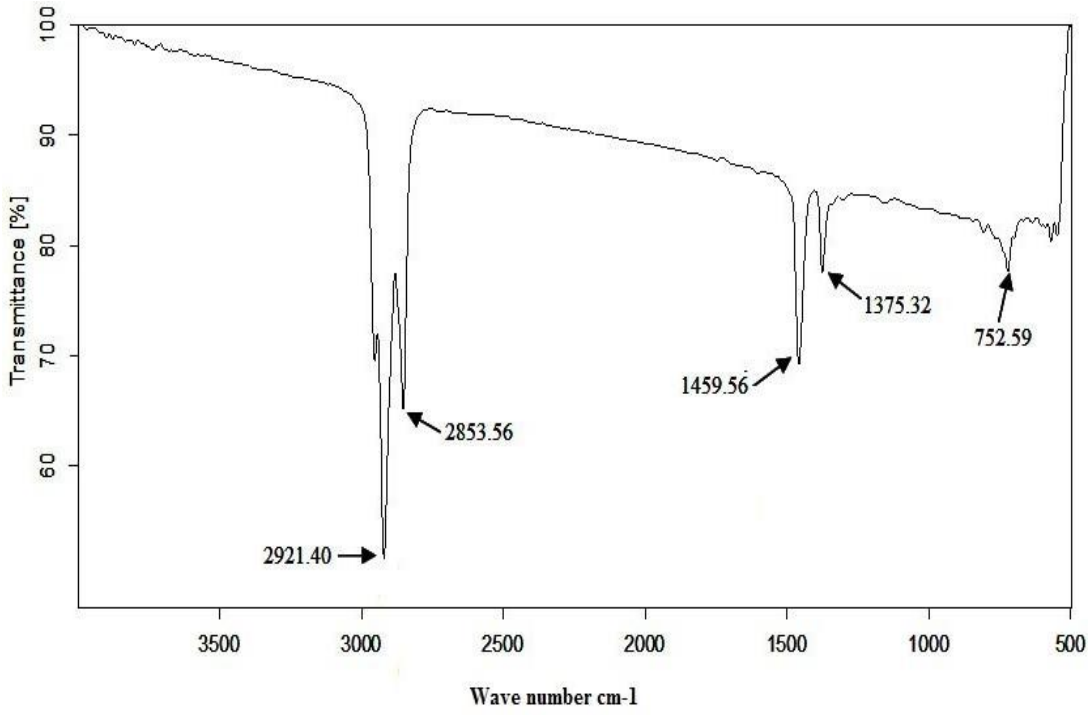

Fig. 5. FTIR spectroscopy of Diesel fuel

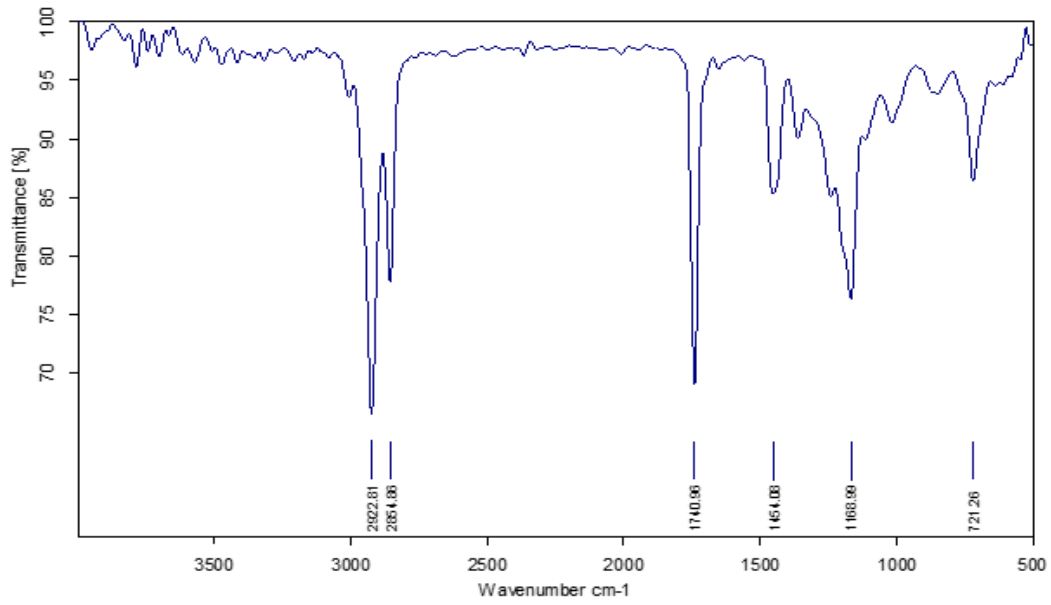

Fig.6. FTIR Spectroscopy PPO20B10GO90 Nanofuel blends

In the spectra about 1650 and 1600 cm-1, the C-C double-bonded structural vibration stretches moderately. Observe this vibration. Stretching vibration from the C-H bend and constriction of the Cracking of a polymer involves the break of C-C bond and formation of new C-H bonds. Also one C-C bond is converted to C=C groups generate the second peak, which may be between 1465 and 1450 cm-1. Ester and tertiary alcohols in the PPO20B10GO90 Nanofuel blend exhibit the C–O stretching pattern at 1210-1163 and 1205-1124 nm. Due to these components, PPO20B10GO90 nanofuel mixes burn better than diesel.

11. Analysis of thermogravimetric (TGA)

Additionally, a thermo-gravimetric evaluation of PPO20B10GO90 Nanofuel blends was also conducted in *air and nitrogen* environments at a rate of increase of 20 degrees Celsius per minute in order to guarantee the thermal and oxidative stabilities of the blends (Figs. 7 and 8). Analyses have shown that mixtures of PPO20B10GO90 Nanofuel are stable up to 150 degrees Celsius and above 275 degrees Celsius (Fig. 6). Nanofuel mixtures like PPO20B10GO90 provide a very minor acceleration to the first mass shift. Figures 6 and 7 show the DTG curves for PPO20B10GO90 and diesel, respectively, for nanofuel mixes. Within the temperature range that was indicated, the greater proportion of shift in mass for PPO20B10GO90 Nanofuel blends implies stronger features of thermos-chemical conversion achieved by fast thermal degradation.

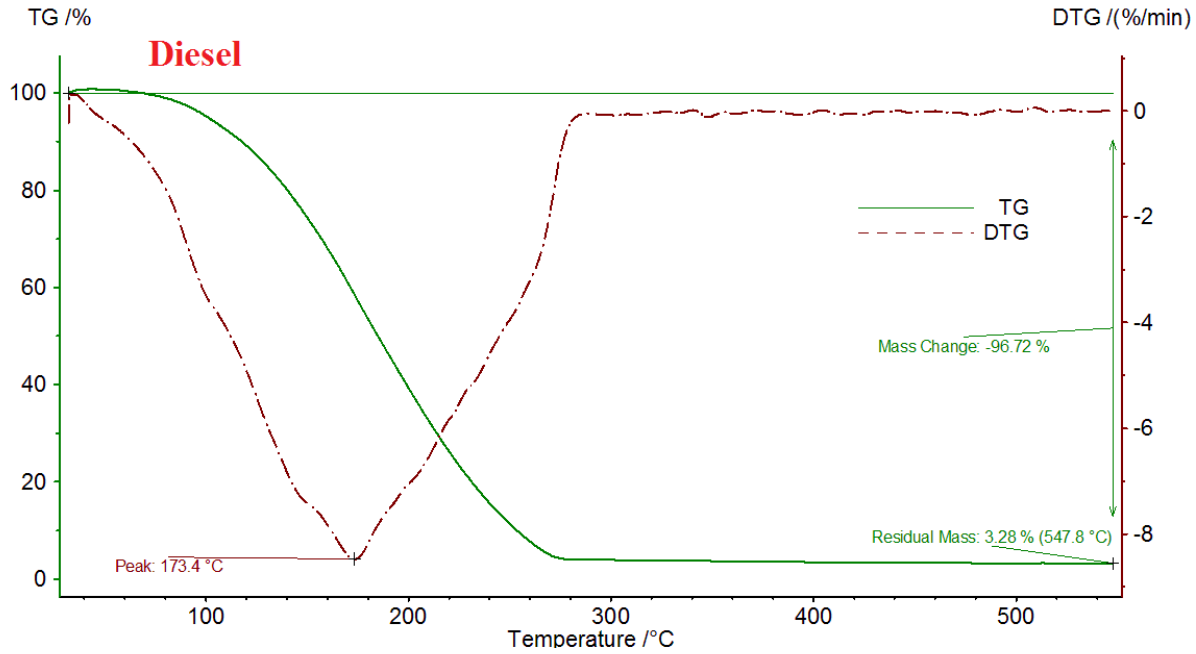

Fig. 7. TGA of Diesel.

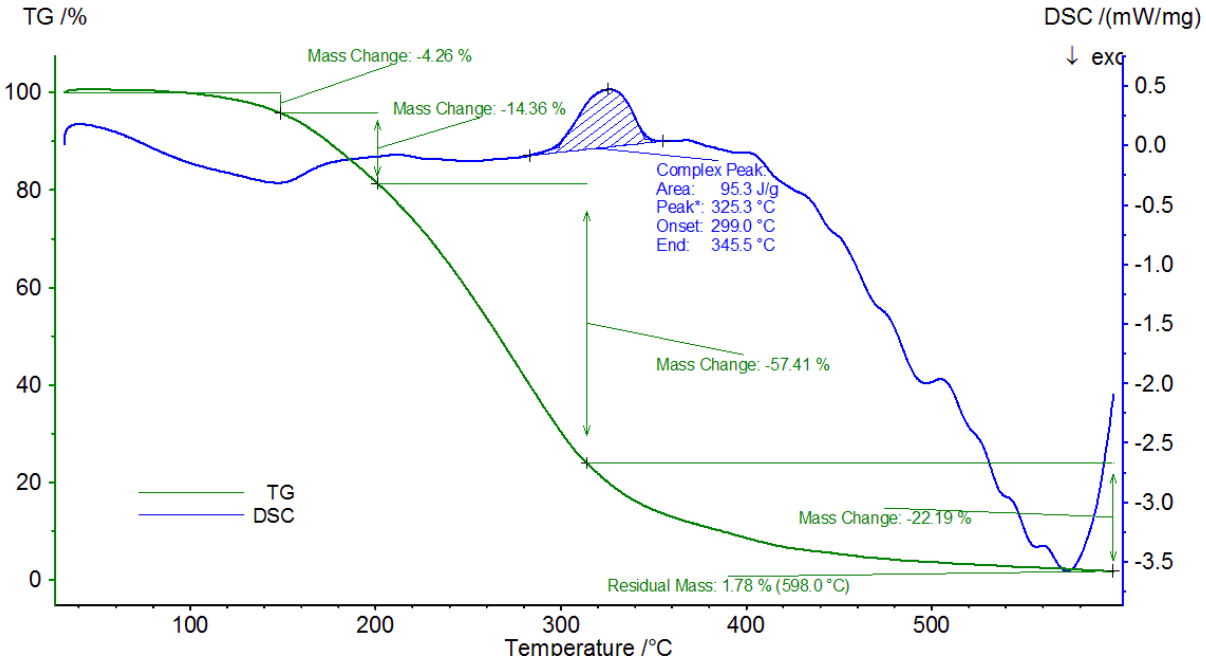

Fig. 8. TGA of PPO20B10GO90 Nanofuel blends

It has been determined through analysis (Fig. 6) that PPO20B10GO90 Nanofuel blends are stable at temperatures over 275 degrees Celsius and below 150 degrees Celsius. The initial mass transition is sped up very slightly by using nanofuel blends like PPO20B10GO90. PPO20B10GO90 and diesel nanofuel blends' DTG curves are depicted in Figure 7 and Figure 8, respectively. PPO20B10GO90 Nanofuel blends show a larger proportional mass shift within the stated temperature range, suggesting stronger thermos-chemical conversion properties via rapid thermal breakdown.

12. Result and discussions

12.1 Features of CRDI Engine Combustion

12.1.1 The Influence that Fuel Additives on the Cylinder Pressure (CP)

Diesel engines' optimal cylinder pressure depends on fuel consumption during pre-mixed combustion. Angle between compression and horsepower strokes impacts CP. The amount of PPO20B10GO90 Nanofuel burned in an uncontrolled combustion engine is directly related to the pressure inside the cylinders. See Figure 8 for the crank angle formulation of cylinder pressure fluctuation during full load.

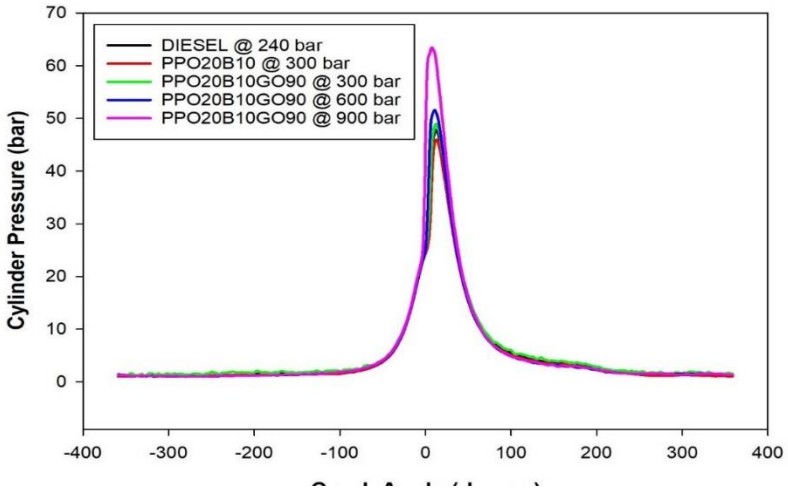

Fig.9 Full-load cylinder pressure and crank angle variations for all test fuels.

GO Nanoparticles at 90 mg/L and 10% n-butanol produced a large volume-to-asymmetric surface-area ratio. produced more oxygen and cetane. They outperformed the other nanofuel mixture

12.1.2 The Fuel Additives' Heat Release Rate

In the Combustion Delay phase, fuel vaporisation and cylinder wall heat loss lower HRR. Two factors contribute to nanofuel blends' improved HRR across the board. These include faster identification and a higher cetane number. Together, these two traits boost engine efficiency [42–45]. Figure 9 shows full-load HRR measurements and crank angle inconsistencies.

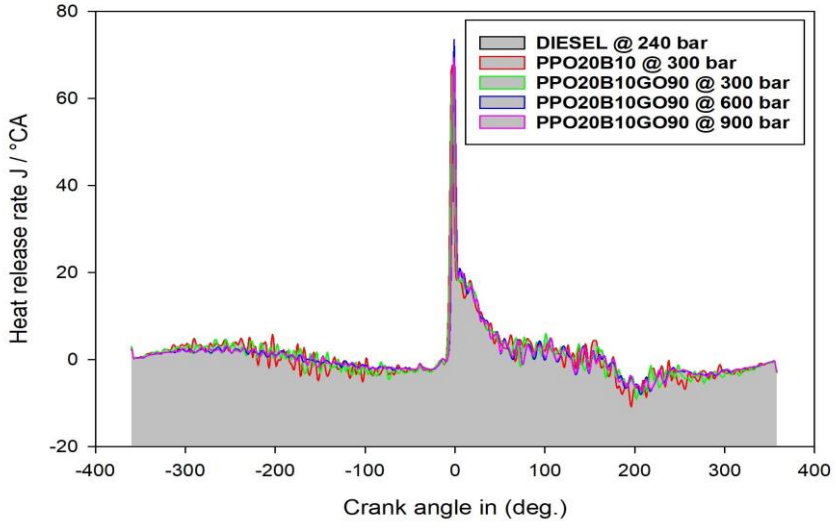

Fig.10 Test fuels' effects on HRR and crank angle at maximum load.

Lower HRR is due to PPO20's higher molecular weight and slower burning velocity [46]. Due to their higher surface area to volume ratio, fast ignition, and improved fuel characteristics and thermal conductivity, nanofuel mixes increase HRR. This causes abnormally high peak pressures. Both HRR and increase. The greatest PPO20B10 GO, diesel,

and PPO20 J/CA were 90.54, 91.997, and 60.813, respectively. Following addition HRR of a combination with pure PPO20 and 90 Parts per million GO and 10% volume n-butanol differed by 29.727 J/CA.

12.1.3 Implications of Ignition Delay (ID) Period Modifiers in Fuel Blends

In the combustion chamber, the chemical delay from pre-combustion processes and the physical delay from vaporisation, atomization, and blending account for ID [48]. Pre-combustion processes result from chemical delay. Fuel-air mixture vaporises by physical delay. Starting the reaction requires ending fuel-air pre-combustion processes, which causes the chemical delay. Figure 10 illustrates rising braking power with shorter ignition delays. Graph shows this pattern.

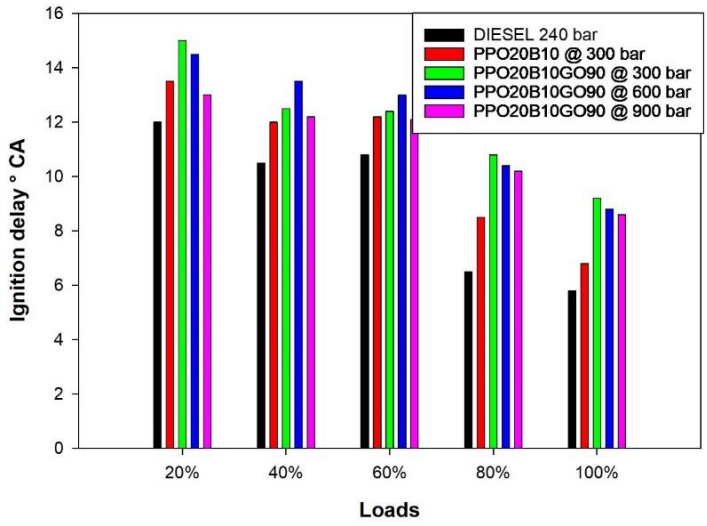

Fig.11. Test fuels with varying maximum loads and ignition delay times, and braking power variations.

The most adverse fuel quality is caused by (PPO20), which results in the longest delay. The PPO with 90 Parts per million GO NPs and Ten % n-butanol had values that were more comparable to diesel as a result of its superior combustion. The ID of PPO20 (10.2 °CA) was much longer than that of PPO20B10GO90 (8.11 °CA), which may be because PPO20 has a greater viscosity. The ignition delay causes an increase in engine temperature, which accelerates and symmetrically burns all mixes, resulting in a reduction in the amount of braking power available. [15]. Mixing of air and fuel results in improved combustion via secondary atomization and microexplosion, which results in a decrease in ID. When loaded, diesel fuel has an ID that is 4.45 CA lower than when it is unloaded. Regardless of the load, Diesel and PPO20B10GO90 fuel mixtures displayed ID times that were identical.12. Features of Engine Efficiency.

13.1 Fuel additive' impact on brake thermal efficiency (BTE)

BTE monitors engine stress by turning fuel thermal energy into mechanical power. BTEs for boosted CRDI diesel engines receive graphene oxide NP doses under constant load. Graphic 12. Except for PPO fuel blends, carbon-based nanoparticle oxides promote fuel charge combustion. Oxygen-buffering graphene oxide improves BTE. The graphene NPs improve BTE. With 90 ppm GO NPs and 10% n-butanol, Mahua biodiesel outperformed clean PPO20B10 at maximum load by 19.37% [30]. At 120 ppm of asymmetric GO NPs, the fuel mix becomes more viscous and dense. PPO20B10GO90 nanofuel blends have diesel-like BTE. BTE increases for all nanofuel pairings under certain loads due to PPO20B10, GO NPs' higher catalytic activity and symmetric micro-explosions.

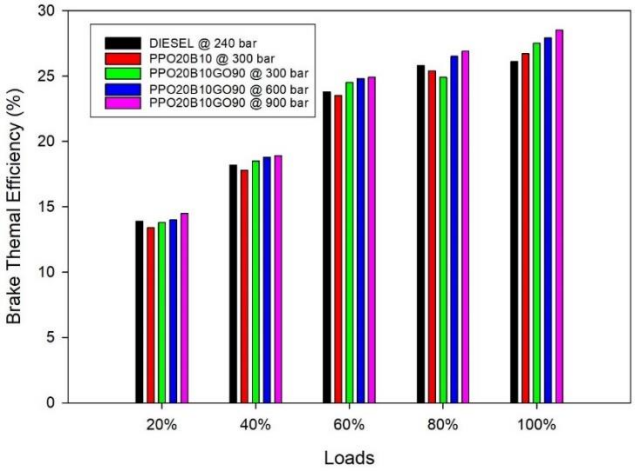

Fig.12. Brake Thermal Efficiency Vs Loads.

12.2 The Impact of Additives on BSFC (Brake-Specific Fuel Consumption)

BSFC is a CRDI diesel engine's ability to provide shaft power and completely burn fuel. This is the fuel-to-electricity ratio. Fuel mix cetane rating is a major factor in ignition delay. Therefore, diesel fuel's cetane number is crucial to CD. Fuel atomization and kinematics viscosity and density are paradoxical.

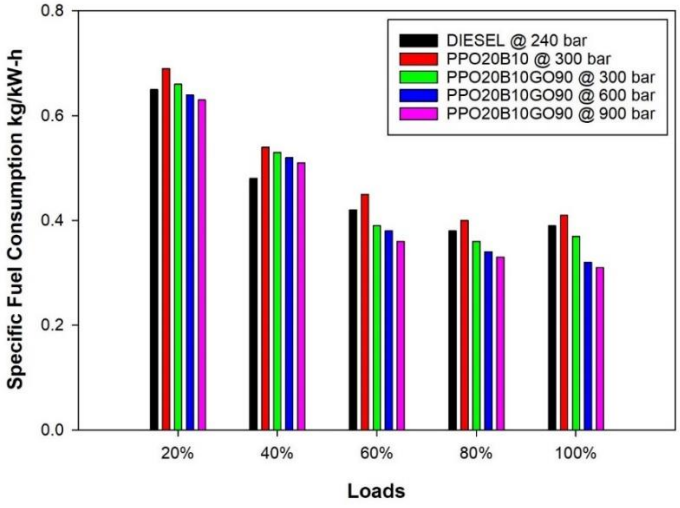

Fig. 13. BSFC vs Injection Pressure.

Figure 12 shows the BP changes for BSFC full loads targeting different fuel mixtures. Poor fuel atomization is caused by PPO20 blends' high viscosity and density. Although n-butanol increases viscosity, it also increases calorie content and cetane number by facilitating more complete burning. High enzyme capacity and sensitive surface area make GO NPs amplify microexplosions [25]. PPO20 additives increase combustion and reduce fueling. The PPO20B10 GO 90 ppm GO has fully loaded BSFCs of 312, 345, and 258 g/kWh.

13. Traits of Emissions Produced by Engines

13.1 The Impact of Fuel Additives and Emissions of Carbon Monoxide (CO)

The incomplete and uneven fuel oxidation in the combustion chamber causes carbon monoxide emissions. For quick acceleration and engine starting, a strong A:F ratio is necessary, leading to CO generation. Since hydrocarbons lack oxygen, they can convert ambient CO_2 into CO. The test's CO and BP range is in Figure 14.

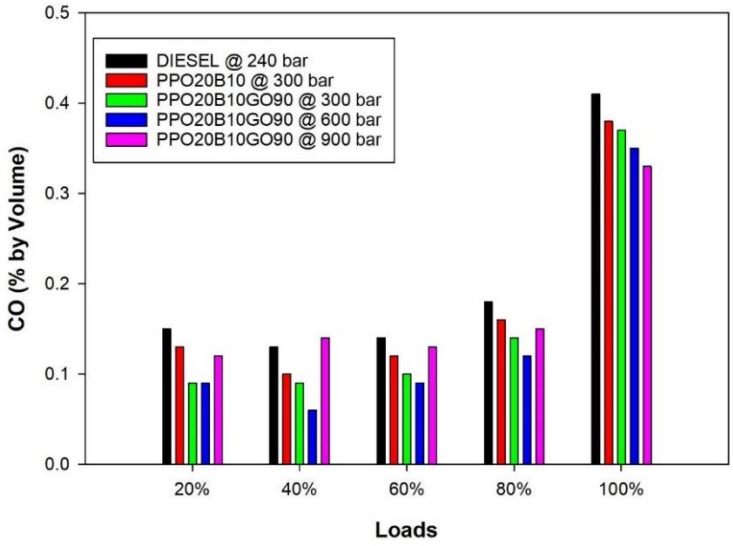

Figure 14: Emission of Carbon Monoxide.

Diesel's low density, high calorie content, and high heat release allowed efficient fuel burning and minimised CO emissions [23,59]. High density, viscosity, and low combustion rate caused PPO20 to emit too much CO into the atmosphere. Its rich A:F ratio, low combustion chamber oxygen, high density, and high viscosity created this. Combining oxide-based asymmetric graphene nanoparticles with butanol accelerates burning [57]. PPO20's graphene oxide and butanol maximise fuel oxidation, burning, heat production, and combustion chamber cooling. The CO emissions of PPO20B10+GO 90 ppm were 54.15 percent lower than PPO20. At 90 ppm GO, PPO20 emitted CO_2 like diesel. With GO NPs and n-butanol, CO emissions can be transformed to harmless CO_2.

13.2 The impact of Fuel Additives on Hydrocarbon (HC) Emissions

Fuels with graphene oxide nanoparticles burn carbon atoms in the combustion area at cylinder wall temperature [51,60]. This lowers nanofuel mix hydrocarbon (HC) emissions. Figure 15 shows how hydrocarbon emissions and braking power fluctuated during the test.

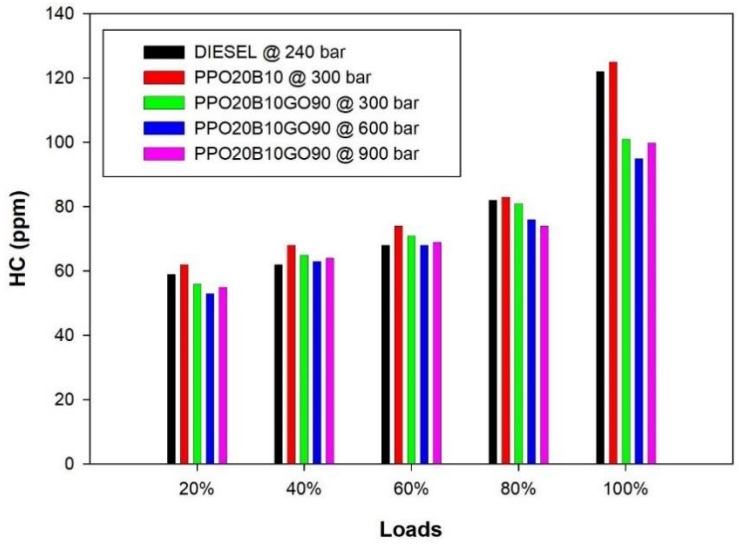

Figure 15: Emission of Hydrocarbons

Hydrocarbon emissions were significantly lower with (PPO20) than with bio diesel, 10% butanol, and GO NP. HC emissions were lowest in PPO20B10GO90. 10% butanol with 90 ppm GO NPs produced 0.0048 g/kWh HC emissions at maximum speed. Lower than plain diesel's HC emissions by 0.00025 g/kWh and PPO20's by 0.2842. HC emissions down 44.72% from diesel and PPO20. The combustion chamber's increased catalytic activity speeds up the burning of asymmetric fuel and air particles.

13.3 The Impact of Fuel Additives on CO_2 Emissions

Plastic pyrolysis oil (PPO20) with graphene oxide nanoparticles emits less CO_2 than PPO20B10GO90. At 80% and 100% load, unburned HC increased CO2 emissions. Hydrocarbons burn to release CO2 and water vapour. Carbon dioxide emissions and braking force from the test fuel mixture are shown in Figure 16. Adding 10% n-butanol to the fuel mixture improves combustion at lower engine and combustion chamber temperatures.

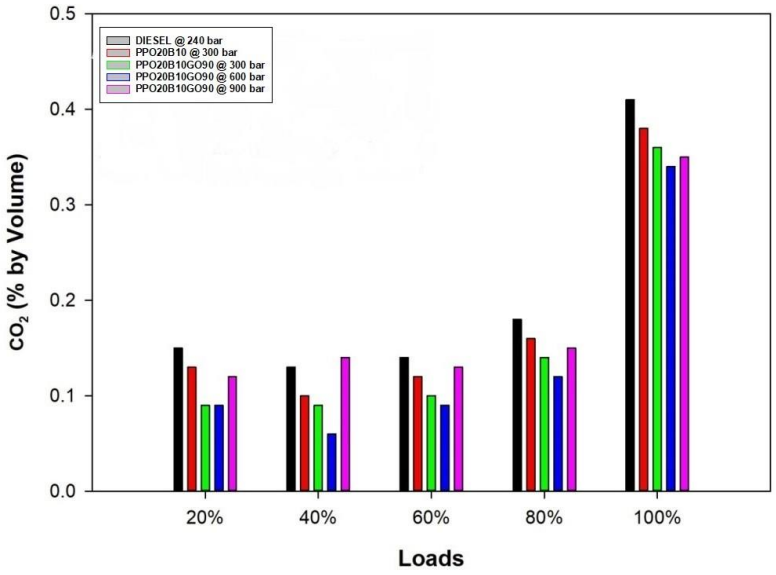

Fig. 16. Emission of Carbon dioxide

The buildup of n-butanol allows this. Better oxidation means the PPO20B10GO90 fuel blend is being burned completely if its CO2 emissions are comparable to diesel fuel at higher loads and burning rates. Running at full capacity with nanofuel blends NSME25B10GO90 produced less CO2 than PPO20. Insufficient (PPO20) combustion produced the most carbon dioxide

13.4 The impact of fuel additives and Nitrogen oxide (NOx) emissions

Nitrogen oxide production is most affected by combustion chamber temperature and O_2 levels. Figure 17 shows the braking power and NOx variations. While testing, some modifications occurred. The study found that PPO20B10 (GO-90 ppm) emit more NOx than diesel.

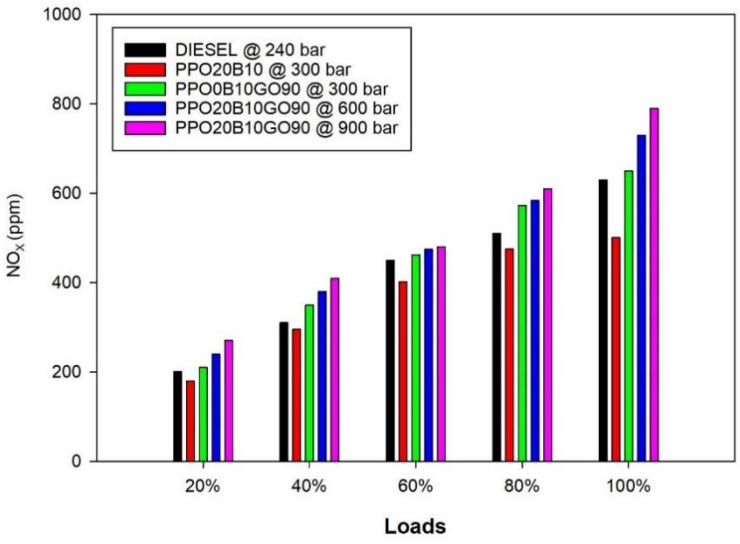

Fig 17: Emission of Nitrous Oxides.

High NOx emissions may result from excessive oxygen molecules, a stabilising substance (Ten % butanol), and various dosages of GO NPs, which provide additional O2 atoms. All of them make high NOx emissions possible. Perhaps all of these factors are involved. This occurrence may potentially boost NOx emissions due to cylinder peak pressure. High NOx emissions are due to this event. PPO20B10GO(90) emits the most NOx, 785 ppm, compared to diesel's 800 ppm and PPO20's 815 ppm. Because of its high ratio of oxygen-donating GO NPs and butanol, it possesses this feature.

13.5 The Impact of Smoke-Producing Fuel Additives

Graphene oxide nanoparticles have an asymmetric surface area of 180 m^2/g, which enables them to activate molecules of air and fuel [3]. Figure 18 illustrates the influence that PPO20B10GO90 Nanofuel mixes have on smoke and braking power. smoke and the ability to halt movement.

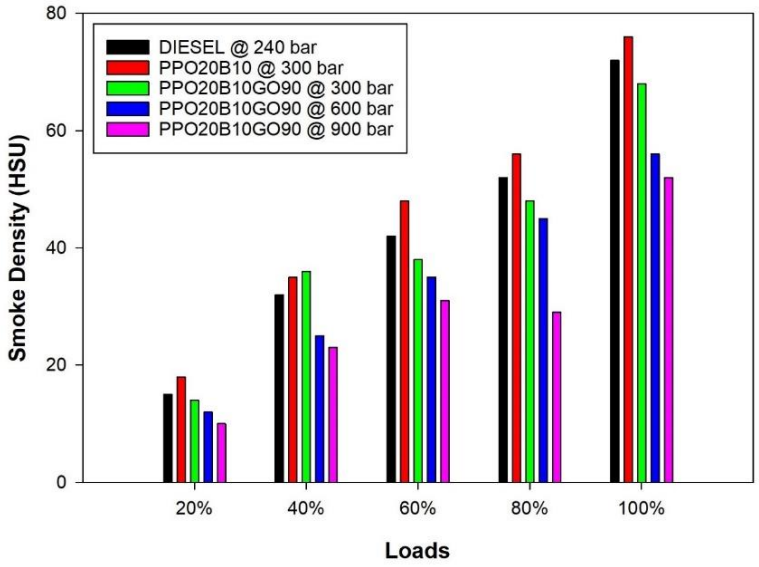

Fig. 18. Smoke Density

Graphene oxide NPs have higher thermal conductivity than other nanoparticles, allowing them to heat each combustion byproduct molecule on the additive surface. Graphene oxide NPs transmit 5000 W/mK. Higher oxygen concentration, lower viscosity, and lower boiling point improve atomization, combustion, and smoke in butanol. The combustion chamber receives more smoke at full load. The smoke emissions of PPO20B10GO90 were equivalent to diesel fuel (72.85 HSU) and PPO20 (70.55 HSU). Nanofuel mixtures lowered smoke output by accelerating premixed combustion due to their shorter ID time.

Conclusions

The thermal cracking technique under oxidizing conditions successfully utilized plastic medical wastes as a possible feedstock for liquid fuel oil. In pyrolysis, the feedstock is bio medical waste plastic with Neyvely Lignite Flay Ash was modified by being re-fuxed with a 3 N NaOH or 3 N H_2SO_4 solution cat/pol = 0.20 The feedstock was thermally

fractured at 773±10 K to recover liquid oil from medical waste, yielding 52 wt%. The liquid oil produced has a gross calorific value of 41 MJ/kg, similar to commercial fuel oils.

Chemical ingredients in liquid fuel oil were analyzed using FTIR spectroscopy to determine their functional groups. The spectrum highlights significant stretching and bending vibrations for alkane, alkene, methylene, alcohol, and ester groups. The liquid oil's chemical properties reveal a composite of damaged and non-degraded organic components from medical mixed plastic wastes. The GC-MS investigation revealed both deteriorated and non-degraded polymeric components in the fuel oil.

Experimental research on the CRDI engine with a toroid-shaped combustion chamber and three-hole fuel injector. A 10% oxygenated addition called N-butanol was added to plastic pyrolysis oil and graphene oxide nanoparticles to lower their viscosity and increase their cetane numbers. It accelerated microexplosions and acted as a catalyst. The effects of bio medical waste plastic pyrolysis oil (PPO20) on CRDI engines are summarised below. plastic pyrolysis oil is mixing diesel, n-butanol, and asymmetric graphene oxide nanoparticles.

Compared to PPO20B10, PPO20 (n-butanol and graphene oxide nanoparticles emulsion fuel) has a substantially greater BTE. PPO20B10GO90 possesses diesel-like BTE. The BTE concentration of PPO20B10GO90 diesel is 19.47% higher than PPO20. GO NPs catalyse all nanofuel blends, improving BTE.

Oxygenated n-butanol nanofuel blends had lower BSFC values due to full fuel combustion and a greater air-to-fuel mixing ratio. Cylinder temperature and oxygen increased.

The toroidal combustion chamber's enhanced air-to-fuel mixing increased heat release and cylinder pressure. Due to swirling motion improvements and a 900 bar 3-hole fuel injector, this was possible. The PPO20, n-butanol, and GO NPs fuel combination caused higher NOx emissions than the PPO20 and diesel-powered vehicles. Fuel types may explain these variances. Due to elevated combustion chamber temperatures, oxygen molecules excess contributed to higher NOx emissions. Meanwhile, the PPO20B10GO90 had the highest NOx emissions of all the tested cars.

After adding GO NPs to PPO20, smoke, CO_2, and HC emissions decreased dramatically. Compared to the PPO20B10 fuel mix, the PPO20B10GO90 fuel blend reduced smoke emissions by 33.85%, nitrogen oxides by 49.83%, and CO emissions by 47.83% at maximum load.

Nomenclature

NPs	Nanoparticles
CRDI	Common rail direct injection
HDPE	High Density Polyethylene
PPO	Plastic pyrolysis oil
SCR	Selective catalytic reaction
DEF	Diesel exhaust fluid

GO	Graphene oxide
SDBS	Sodium dodecyl benzene sulphonate
nm	Nanometer
HRR	Heat release rate
BTE	Brake thermal efficiency
ppm	Parts per million
HC	Hydrocarbon
CO2	Carbon dioxide
CO	Carbon monoxide
NOX	Oxides of nitrogen
PM	Particulate matter
BSFC	Brake-specific fuel consumption

References

1. Mani M, Subash C, Nagarajan G. Performance, emission and combustion characteristics of a DI diesel
   engine using waste plastic oil. Applied Thermal Engineering. 2009;29(13):2738-2744. 2003, 37 (22), 5135−5142.
2. Kumar S, Singh RK. Recovery of hydrocarbon liquid from waste high density polyethylene by thermal pyrolysis. Braz J Chem Eng 2011;28(04):659–67.
3. Mani M, Nagarajan G. Influence of injection timing on performance, emission and combustion characteristics of a DI diesel engine running on waste plastic oil. Energy 2009;34:1617–23.
4. Wallis MD, Bhatia SK. Thermal degradation ofhigh density polyethylene in a reactive extruder. Polym Degrad Stabil 2007;92:1721–9.
5. Consea JA, Font R, Marcilla A, Garcia AN. Pyrolysis of polyethylene in a fluidized bedreactor. Energy Fuel 1994;8:1238–46.
6. Walendziewski J, Steininger M. Thermal and catalytic conversion of waste polyolefins. Catal Today 2001;65:323–30.
7. Beltrame PL, Carniti P, Audisio G, Bertini F. Catalytic degradation of polymers. Part II – Degradation of polyethylene. Polym Degrad Stabil 1989;26:209–20.
8. Bagri R, Williams PT. Catalytic pyrolysis of polyethylene. J Anal Appl Pyrol 2002;63:29–41.
9. Venuto PB, Habib ET. Fluid catalytic cracking with zeolite catalysts. New York: Marcel Dekker Inc.; 1979.
10. Sharratt PN, Lin YH, Garforth AA, Dwyer J. Investigation of the catalytic pyrolysis of high-density polyethylene over a HZSM-5 catalyst in a laboratory fluidized-bed reactor. Indus Eng Chem Res 1997;36(5):118–24.
11. Miskolczi N, Bartha L. Investigation of hydrocarbon fractions form waste plastic recycling by FTIR, GC, EDX RFS and SEC techniques. J Biochem Bioph Meth 2008;70:1247–53.
12. Seo YH, Lee KH, Shin DH. Investigation of catalytic degradation of high-density polyethylene by hydrocarbon group type analysis. J Anal Appl Pyrol 2003;70:383–98.

13. Park JW, Kim JH, Seo G. The effect of pore shape on the catalytic performance of zeolites in the liquid-phase degradation of HDPE. Polym Degrad Stabil 2002;76:495–501.
14. Panda AK, Singh RK. Catalytic performances of kaoline and silica alumina in the thermal degradation of polypropylene. J Fuel Chem Technol 2011;39(3):198–202.
15. Panda AK, Singh RK, Mishra DK. Thermo-catalytic degradation of thermocol waste to value added liquid products. Asian J Chem 2012;24(12):5539–42.
16. Usta N. An experimental study on performance and exhaust emissions of a diesel engine fuelled with tobacco seed oil methyl ester. Energy Convers Manage 2005;46:2373–86.
17. Shakal, J. and Martin, J. K., "Effects of Auxiliary Injection on Diesel Engine Combustion," SAE Paper 900398, 1990.
18. Shundoh, S., et al., "NOx Reduction from Diesel Combustion Using Pilot Injection with High Pressure Fuel Injection," SAE Paper 920461, 1992.
19. D. A. Nehmerand R. D. Reitz, “Measurement of the Effect of Injection Rate and Split Injections on Diesel Engine Soot and NOx Emissions”, DOI: https://doi.org/10.4271/940668, SAE PAPER 940668, 1994
20. Erhard Sitter, Fuel Injection Apparatus With Plot Njection And Man Injection N Internal Combustion Engines, United States Patent US4520774A
21. Gan, Y.; Qiao, L. Combustion characteristics of fuel droplets with addition of nano and micron-sized aluminum particles. Combust. Flame 2011, 158 (2), 354−368.
22. Chehroudi, B. Nanotechnology and Applied Combustion: Use of Nanostructured Materials for Light-Activated Distributed Ignition of Fuels with Propulsion Applications. Recent Patents on Space Technology 2011, 1 (2), 107−122.
23. Mehta, R. N.; Chakraborty, M.; Parikh, P. A. Nanofuels: Combustion, engine performance and emissions. Fuel 2014, 120 (0), 91−97.
24. Sudheer nandi, “ Performance of CI Engine by using biodiesel-Mahua oil ”, American Journal of Engineering Research, vol 02, issue 10, pp. 22-47
25. Pope, C. A., Burnett, R. T.; Thun, M. J.; Calle, E. E.; Krewski, D.; Ito, K.; Thurston, G. D. Lung cancer, cardiopulmonary mortality, and long-term exposure to fine particulate air pollution. Jama 2002, 287 (9), 1132−1141.
26. Sharifi, S.; Behzadi, S.; Laurent, S.; Laird Forrest, M.; Stroeve, P.; Mahmoudi, M. Toxicity of nanomaterials. Chem. Soc. Rev. 2012, 41 (6), 2323−2343.
27. Kim, F.; Luo, J.; Cruz-Silva, R.; Cote, L. J.; Sohn, K.; Huang, J. Self-Propagating Domino-like Reactions in Oxidized Graphite. Adv. Funct. Mater. 2010, 20 (17), 2867−2873.
28. Li, J.-L.; Kudin, K. N.; McAllister, M. J.; Prud’homme, R. K.; Aksay, I. A.; Car, R. Oxygen-Driven Unzipping of Graphitic Materials. Phys. Rev. Lett. 2006, 96 (17), 176101.
29. Zhu, Y.; Murali, S.; Cai, W.; Li, X.; Suk, J. W.; Potts, J. R.; Ruoff, R. S. Graphene and graphene oxide: synthesis, properties, and applications. Adv. Mater. 2010, 22 (35), 3906−3924.
30. Ahmed I. El-Seesy, Hamdy Hassan , S. Ookawara, “Effects of graphene nanoplatelet addition to jatropha BiodieseleDiesel mixture on the performance and emission characteristics of a diesel engine”, https://doi.org/10.1016/j.energy.2018.01.108, Volume 147, 15, Pages 1129-1152, 2018
31. A.I. EL-Seesy, H. Hassan, S. Ookawara, Performance, combustion, and emission characteristics of a diesel engine fueled with Jatropha methyl ester and graphene oxide

additives, Energy Convers. Manag. 166 (2018) 674–686, https://doi.org/10. 1016/j.enconman.2018.04.049.

32. Jong Boon Ooi , Harun Mohamed Ismail , Boon Thong Tan a , Xin Wang "Effects of Graphite Oxide and Single-Walled Carbon Nanotubes as 2 Diesel Additives on the Performance, Combustion, and Emission 3 Characteristics of a Light-Duty Diesel Engine", Renewable Energy, https://doi.org/10.1016/j.energy.2018.07.062, Volume 161, 15, Pages 70-80, October 2018
33. S.S. Hoseini, G. Najafi, B. Ghobadian, R. Mamat, M.T. Ebadi, T. Yusaf "Novel environmentally friendly fuel: The effects of nanographene oxide additives on the performance and emission characteristics of diesel engines fuelled with Ailanthus altissima biodiesel", Renewable Energy, https://doi.org/10.1016/j.renene.2018.02.104, Volume 125, , Pages 283-294, 2018
34. Ahmed I. EL-Seesya,b, HamdyHassana,c, "Investigation of the Effect of Adding Graphene Oxide, Graphene 2 Nanoplatelet, and Multiwalled Carbon Nanotube Additives with n3 Butanol-Jatropha Methyl Ester on a diesel engine performance", Renewable Energy, DOI:10.1016/j.renene.2018.08.026, 2018
35. Luis Tipanluisaa,d , Natalia Fonseca , Jesús Casanova , Jos´e-María Lopez, "Effect of n-butanol/diesel blends on performance and emissions of a heavy-duty diesel engine tested under the World Harmonised Steady-State cycle" , Fuel, https://doi.org/10.1016/j.fuel.2021.121204Volume 302, 15, 121204, October 2021
36. K. Siva Prasad, S. Srinivasa Rao & V.R.K. Raju "Performance and emission characteristics of a DICI engine operated with n-butanol/diesel blends" , Energy Sources, Part A: Recovery, Utilization, And Environmental Effects https://doi.org/10.1080/15567036.2019.1685611, 2019
37. Ashish Nayyar , Dilip Sharma , Shyam Lal Soni , Alok Mathur , Experimental investigation of performance and emissions of a VCR diesel engine fuelled with n-butanol diesel blends under varying engine parameters. Environ Sci Pollut Res 24:20315–29. doi:10.1007/s11356-017-9599-8.
38. Nadir Yilmaz , Francisco M. Vigil, Kyle Benalil, Stephen M. Davis, Antonio Calva "Effect of biodiesel–butanol fuel blends on emissions and performance characteristics of a diesel engine", Feul, https://doi.org/10.1016/j.fuel.2014.06.022, Volume 135, 1 Pages 46-50, November 2014
39. S.Imtenan, H.H.MasjukiM.VarmanI.M.Rizwanul FattahH.SajjadM.I.Arbab "Effect of n-butanol and diethyl ether as oxygenated additives on combustion–emission-performance characteristics of a multiple cylinder diesel engine fuelled with diesel–jatropha biodiesel blend", Energy Conversion and Management, https://doi.org/10.1016/j.enconman.2015.01.047, Volume 94, , Pages 84-94, April 2015
40. Dimitrios C. Rakopoulos , Constantine D. Rakopoulos , Evangelos G. Giakoumis , Roussos G. Papagiannakis , Dimitrios C. Kyritsis c, "Influence of properties of various common bio-fuels on the combustion and emission characteristics of high-speed DI (direct injection) diesel engine: Vegetable oil, bio-diesel, ethanol, n-butanol, diethyl ether", Energy, DOI:10.1016/j.energy.2014.06.032
41. Atmanli A, Yuksel B, Ileri E ,"Experimental investigation of the effect of diesel–cotton oil–n-butanol ternary blends on phase stability, engine performance and exhaust emission

parameters in a diesel engine"., Fuel, https://doi.org/10.1016/j.fuel.2013.03.012 109:503–511, Volume 109, July 2013, Pages 503-511

42. Atmanli A, Ileri E, Yuksel B " Experimental investigation of engine performance and exhaust emissions of a diesel engine fueled with diesel–n-butanol–vegetable oil blends". Energy Conversion and Management, https://doi.org/10.1016/j.enconman.2014.02.049, Volume 81, May 2014, Pages 312-321
43. Atmanli A, Ileri E, Yuksel B, Yilmaz N,Extensive analyses of diesel–vegetable oil–n-butanol ternary blends in a diesel engine. Applied Energy, https://doi.org/10.1016/j.apenergy.2015.01.071 , Volume 145, 1 May 2015, Pages 155-162
44. Manzoore Elahi. M. Soudagara,, Nik-Nazri Nik-Ghazalia,, M.A. Kalama , Irfan Anjum Badruddinb , N.R. Banapurmathc , T.M. YunusKhanb , M. Nasir Bashira , Naveed Akrama , RijavanFaraded , Asif Afzale "The effects of graphene oxide nanoparticle additive stably dispersed in dairy scum oil biodiesel-diesel fuel blend on CI engine: performance, emission and combustion characteristics", Fuel, https://doi.org/10.1016/j.fuel.2019.116015Volume 257, 1 December 2019, 116015
45. S.S. Hoseini , G. Najafi a, B. Ghobadian , M.T. Ebadi , R. Mamat , T. Yusaf , "Biodiesels from three feedstock: The effect of graphene oxide (GO) nanoparticles diesel engine parameters fuelled with biodiesel", Renewable Energy, https://doi.org/10.1016/j.renene.2019.06.020, Volume 145, January 2020, Pages 190-201
46. S.S. Hoseini , G. Najafi a, B. Ghobadian a , M.T. Ebadi a , R. Mamat b , T. Yusaf, "Performance and emission characteristics of a CI engine using graphene oxide (GO) nano-particles additives in biodiesel-diesel blends", Renewable Energy https://doi.org/10.1016/j.renene.2019.06.006, Volume 145, January 2020, Pages 458-465
47. Sabourin, J. L.; Dabbs, D. M.; Yetter, R. A.; Dryer, F. L.; Aksay, I. A. Functionalized graphene sheet colloids for enhanced fuel/ propellant combustion. ACS Nano 2009, 3 (12), 3945−3954.
48. D.K.Bora, M.pally, V.Sanduja, "Performance evaluation and emission characteristics of a diesel engine using Mahua oil Methyl ester (MOME).SAE:10.4271/2004-28-0034
49. Freedman B, Pryde EH, Mounts TL. Variables affecting the yields of fatty esters from transesterified vegetable oils. Journal of American Oil Chemists Society 1984;61(10): 1638–43
50. Fangrui MA, Hanna MA. Biodiesel production a review. Bioresource Technology 1999;70(1):1–15.
51. E. Griffin Shay " Diesel Fuel From Vegetable Oils: Status And Opportunities" National Academy of Sciences, 2101 Constitution Avenue, Washington, DC 20418, U.S.A., https://doi.org/10.1016/0961-9534(93)90080-N, Vol. 4, No. 4, pp. 227242, 1993
52. Vijayakumar Chandrasekaran , Murugesan Arthanarisamy b , PanneerselvamNachiappan c , Subramaniam Dhanakotti b , Bharathiraja Moorthy, "The role of nano additives for biodiesel and diesel blended transportation fuels" Transportation Research Part D: Transport and Environment, http://dx.doi.org/10.1016/j.trd.2016.03.015, Volume 46, , Pages 145-156, July 2016
53. Jong Boon Ooi, Harun Mohamed Ismail, Varghese Swamy, Xin Wang, Akshaya Kumar Swain, and Jeevan Raj Rajanren, Graphite Oxide Nanoparticle as a Diesel Fuel Additive for

Cleaner Emissions and Lower Fuel Consumption. https://doi.org/10.1021/acs.energyfuels.5b02162, Energy Fuels 2016, 5, 02162

54. Hurmathulla Khan , Manzoore Elahi M. Soudagar , Rajagopal Harish Kumar , Mohammad Reza Safaei , Muhammad Farooq , AbdulqhadarKhidmatgar , Nagaraj R Banapurmath , Rizwan A. Farade , Muhammad Mujtaba Abbas , Asif Afzal , Waqar Ahmed , MarjanGoodarzi and Syed NoemanTaqui , "Effect of Nano-Graphene Oxide and n-Butanol Fuel Additives Blended with Diesel—Nigella sativa Biodiesel Fuel Emulsion on Diesel Engine Characteristics",*Symmetry* **,** DOI:10.1016/j.fuproc.2020.106406 2020
55. Guoan Li Quan Zhang "Sodium dodecyl benzene sulfonate aqueous solution and preparation method thereof and application", CN101632353B
56. B M Paramashivaiah1 and C R Rajashekhar "Studies on effect of various surfactants on stable dispersion of graphene nano particles in simarouba biodiesel", IOP Conf. Series: Materials Science and Engineering 149 (2016) 012083 doi:10.1088/1757-899X/149/1/012083
57. Wickham, D. T.; Cook, R. L.; Engel, J.; Jones, M.; Nabity, J. Soluble Nanocatalysts for High Performance Fuels.Presented at the 19th ONR Propulsion Meeting, Los Angeles, CA, December 20, 2006.
58. Wickham, D. T.; Cook, R. L.; De Voss, S.; Engel, J. R.; Nabity, J. Soluble Nanocatalysts for High Performance Fuels. J. Russ. Laser Res. 2006, 27, 552–561.
59. Linda Vaisman, H. Daniel Wagner, Gad Marom, The role of surfactants in dispersion of carbon nanotubes, Advances in Colloid and Interface Science 128–130 (2006) 37–46.
60. Richa Rastogi, Rahul Kaushal, S.K. Tripathi, Amit L. Sharma, Inderpreet Kaur, Lalit M. Bharadwaj, Comparative study of carbon nanotube dispersion using surfactants, Journal of Colloid and Interface Science 328 (2008) 421–428.
61. Mondal, B.K., Islam, M.N., Hossain, M.E., et al. 2019. Microstructural and mineralogical properties of acid and alkali activated coal fy ash. Journal of Advanced Chemical Sciences 5 (1): 612–614. https://doi.org/10.30799/jacs.201.19050102.
62. Akter, N., Rahman, M., Sharmin, L., & Team IPSU. Medical waste management at Rajshahi city corporation public private partnership model development: A collaborative efort on medical waste Management in Bangladesh (Baseline and status report). Antrocom Online J. Anthropol. 6 (2), 173–186 (2010).
63. 8. Singh, B. & Nisha, S. Mechanistic implications of plastic degradation. Polym. Degrad. Stab. https://doi.org/10.1016/j.polymdegra dstab.2007.11.008 (2008).